

# Mechanistic Studies of Sanguinamide B Derivatives: A Unique Inhibitor of Eukaryotic Ribosomes

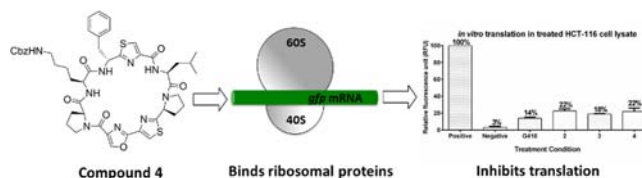
Worawan Tantisantisom, Deborah M. Ramsey, and Shelli R. McAlpine\*

School of Chemistry, The University of New South Wales, Kensington,  
NSW 2052 Australia

s.mcalpine@unsw.edu.au

Received June 20, 2013

## ABSTRACT



Described are mechanistic studies of two Sanguinamide B (San B) derivatives. These compounds were identified as eukaryotic ribosomal inhibitors. Two biotinylated San B derivatives were synthesized and used to capture protein targets in a pull-down assay. LC/MS/MS analysis of the San B-captured targets identified several proteins that comprise eukaryotic ribosomal subunits. The translation inhibitory effect of San B was confirmed using an *in vitro* translation assay. Moreover, an evaluation of cell death mechanisms is reported.

The first total synthesis of the Sanguinamide B<sup>1</sup> (San B; **1**) natural product was described by Singh et al.<sup>2</sup> Singh confirmed the structure of the natural product (*trans, trans*-San B) and identified the thermodynamically stable conformers (*trans, cis*-San B and *cis-cis*-San B). Biological evaluation of San B indicated pilicide activity against *Pseudomonas aeruginosa*, which utilizes type IV pili in biofilm formation.<sup>3</sup> The structure–activity relationships of the San B analogues were explored by synthesizing 12 compounds, whereby we exchanged the valine, alanine, and leucine residues with *N*-methyl, glycine, and L- or D-phenylalanine amino acids.<sup>4</sup> Most of the analogues synthesized had multiple stable conformations, and in some cases a specific conformation exhibited greater bioactivity than the same compound in a different conformation.<sup>4</sup> All 12 San B analogues were tested in cytotoxicity assays against a human colorectal carcinoma cell line (HCT-116).<sup>5</sup> Our data showed that two D-Phe analogues (Figure 1; compounds **2** and **3**) were cytotoxic to HCT-116 cells and reduced cell survival by more than

50% at a 50  $\mu$ M concentration, with IC<sub>50</sub> values of 43  $\pm$  4.8 and 38  $\pm$  2.1  $\mu$ M, respectively.<sup>5</sup>

Herein we report the synthesis of two biotinylated analogs of compounds **2** and **3**: **2-Tag** and **3-Tag**. We show, via pull-down assays, that these two compounds bind to proteins associated with the 40S (small) and 60S (large) ribosomal subunits. The translation inhibitory effect of San B was confirmed using an *in vitro* translation assay. Evaluation of cell death mechanisms in San B-analog treated cells indicates that, in spite of structural similarities, one compound induced necrosis and one induced cell death in a manner resembling autophagy. En route to producing the tagged compound we generated a structurally related third San B derivative. This molecule was the most potent of all the San B analogues published to date, and it induced apoptosis.

Thus, given that none of the other 10 analogs or the natural product were cytotoxic, we felt that a mechanism investigation of compounds **2** and **3** would provide interesting data on how the conformation and structure of these two compounds might dictate their biological activity. We synthesized two biotinylated derivatives: **2-Tag** and **3-Tag** (Figure 1). Our structure–activity relationship (SAR) data<sup>5</sup> indicated that the valine position in the natural

(1) Dalisay, D. S.; Rogers, W. W.; Edison, A. S.; Molinski, T. F. *J. Nat. Prod.* **2009**, 72, 732.

(2) Singh, E.; Ramsey, D. M.; McAlpine, S. R. *Org. Lett.* **2012**, 14, 1198.

(3) Ramsey, D. M.; Wozniak, D. J. *Mol. Microbiol.* **2005**, 56, 309.

(4) Wahyudi, H.; Tantisantisom, W.; Liu, X.; Ramsey, D. M.; Singh, E. K.; McAlpine, S. R. *J. Org. Chem.* **2012**, 77, 10596.

(5) McAlpine unpublished result.

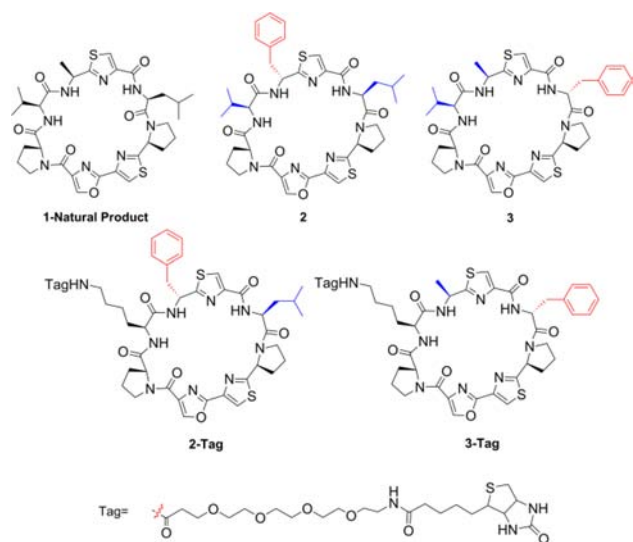
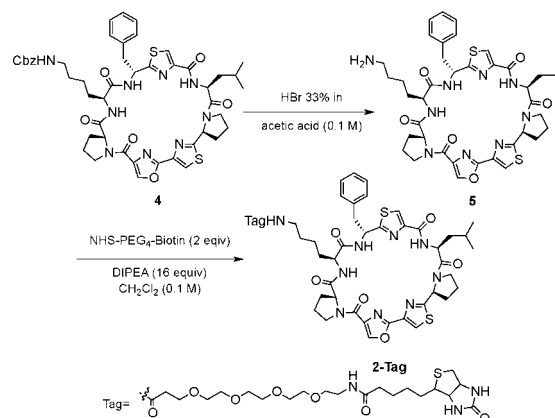


**Figure 1.** San B natural product (**1**),<sup>1–2</sup> San B derivatives (**2–3**),<sup>4</sup> and the biotinylated derivatives, **2-Tag** and **3-Tag**.

product could be substituted without impacting the molecule's potency. Thus, we incorporated the tag at this position for both compounds. En route to both compounds, we synthesized the carboxybenzyl (Cbz) protected lysine derivatives, where compound **4** is the Cbz lysine precursor of **2-Tag**. Compound **4** was tested for its cytotoxicity, and we found that it exhibited an  $IC_{50}$  of  $15.9 \pm 1.3 \mu M$ , which was 2.7-fold more potent than its parent analog scaffold. No cytopathic effect was observed when cells were treated with a  $50 \mu M$  concentration of the Cbz lysine precursor of **3-Tag**.<sup>6</sup> The synthesis of the Cbz-lysine derivatives of compounds **2** and **3** were performed as previously described for other analogues, with the exception that a Cbz-lysine was incorporated into the macrocycle.<sup>4</sup> Biotinylation to generate **2-tag** and **3-tag** was performed by cleavage of the Cbz protecting group using 33% HBr in acetic acid, yielding free lysine. The lysine was readily biotinylated using 2.0 equiv of *N*-hydroxysuccinimide esters—polyethylene glycol (4 units)—Biotin (NHS-PEG<sub>4</sub>-biotin) and 16.0 equiv of *N,N*-Diisopropylethylamine (DIPEA) dissolved in dichloromethane to yield biotinylated San B derivatives (Scheme 1).<sup>7</sup> The biotinylated compounds were utilized in pull-down assays to determine the

compounds' protein target(s), following standardized methods.<sup>7</sup> Proteins were separated by electrophoresis and visualized with Coomassie R-250 staining solution (Figure S4a).<sup>6</sup> Protein sequencing of each band was performed using trypsin digestion and LC/MS/MS sequencing, followed by peptide identification using the NCBI Eukaryotic database and peptide fingerprinting software. The results for compound **3-tag** are shown in Table 1, and similar results were observed for **2-tag**, which pulled-down 60S ribosomal proteins, as well as the eukaryotic elongation factor 2 (Table S2).<sup>6</sup>

#### Scheme 1. Synthesis of San B Biotinylated Tagged Derivatives



San B tagged derivatives captured proteins that are components of ribosomal subunits and play a crucial role in protein synthesis (translation). Cell growth requires protein synthesis to increase the overall biomass of the cell, and malfunction of the translation machinery halts cell cycle progression and leads to cell death.<sup>8</sup> There are numerous factors that comprise the translation machinery, including ribosomal proteins (Bands F, I, J, L–N, Table 1), translation elongation factors (such as elongation factor 2, Band C, Table 1), tRNAs (tRNAs), and energy sources.<sup>9</sup> Ribosomal proteins are formed from the 40S (small) and 60S (large) ribosomal subunits.<sup>10</sup> Our San B **3-tag** derivatives bound proteins from the 40S (S11) and the 60S (L3, 7, 12, 18, 23) subunits, whereas **2-tag** appears to primarily interact with 60S ribosomal subunits (L9, 10, 13, 17).

**Table 1.** Protein Sequencing Results from Pull-down Assays with Compound **3-tag**<sup>a</sup>

band	protein	mass (kDa)	MASCOT score
C	elongation factor 2	95.2	362
F	60S ribosomal proteins L3	45.4	583
I	60S ribosomal protein L7	29.2	386
J	60S ribosomal protein L18a	20.7	400
L	40S ribosomal protein S11	18.4	304
M	60S ribosomal protein L12	17.8	320
N	60S ribosomal protein L23	14.8	278

<sup>a</sup> See Supporting Information for all pull-down data and gels.

(6) See Supporting Information for details.

(7) (a) Vasko, R. C.; Rodriguez, R. A.; Cunningham, C. N.; Ardi, V. C.; Agard, D. A.; McAlpine, S. R. *ACS Med. Chem. Lett.* **2010**, *1*, 4. (b) Ardi, V. C.; Alexander, L. D.; Johnson, V. A.; McAlpine, S. R. *ACS Chem. Biol.* **2011**, *6*, 1357. (c) Kunicki, J. B.; Petersen, M. N.; Alexander, L. D.; Ardi, V. C.; McConnell, J. R.; McAlpine, S. R. *Bioorg. Med. Chem. Lett.* **2011**, *21*, 4716. (d) Ramsey, D. M.; McConnell, J. R.; Alexander, L. D.; Tanaka, K. W.; Vera, C. M.; McAlpine, S. R. *Bioorg. Med. Chem. Lett.* **2012**, *22*, 3287.

(8) (a) Fingar, D. C.; Blenis, J. *Oncogene* **2004**, *23*, 3151. (b) Naora, H. *Immunol. Cell Biol.* **1999**, *77*, 197.

(9) (a) Marintchev, A.; Wagner, G. *Q. Rev. Biophys.* **2004**, *37*, 197. (b) Agirrezabala, X.; Frank, J. *Q. Rev. Biophys.* **2009**, *42*, 159.

(10) (a) Panse, V. G.; Johnson, A. W. *Trends Biochem. Sci.* **2010**, *35*, 260. (b) Voigts-Hoffmann, F.; Klinge, S.; Ban, N. *Curr. Opin. Struct. Biol.* **2012**, *22*, 768.

The similarity in the proteins isolated by both compounds imply that the cytosolic targets of Sanguinamide B are ribosomes.

To verify that compounds **2**, **3**, and **4** act as translation inhibitors, we utilized a cell-free *in vitro* translation assay. Measuring protein synthesis in the presence of the derivatives, as well as comparing the results to a commercially available translational inhibitor (G418),<sup>11</sup> provides evidence on whether our molecules inhibit protein synthesis (Figure 2a). The concentrations of compounds used in the assays were based on the IC<sub>50</sub> values of the compounds.

Using HCT-116 cell lysate as the ribosomal source, we added accessory proteins and monitored the translation of active green fluorescent protein (GFP). The amount of GFP was measured and quantitated by flow cytometry. Relative fluorescence units (RFU) for each reaction were normalized to a positive control, which contained the GFP reporter system but no compounds or translational inhibitors (Figure 2a). Comparing compounds **2**, **3**, and **4** to the positive control, we observe a significant reduction in translation of GFP compared to the positive control. Compound **2** (50  $\mu$ M) reduces translation by 4.5-fold ( $22 \pm 2.4\%$  RFU;  $p < 0.0007$ ), and compound **3** (50  $\mu$ M) by 5.6-fold ( $18 \pm 0.5\%$  RFU;  $p < 0.0001$ ). Compound **4** (20  $\mu$ M) reduced translation by 4.5-fold, but with 2.5 times less compound ( $22 \pm 3.9\%$  RFU;  $p < 0.03$ ). The reduction in GFP translation observed with San B analogues was similar to that observed with the translation inhibitor G418 (5  $\mu$ M) ( $14 \pm 1.4\%$  RFU;  $p < 0.0023$ ). Although the potency of San B derivatives must be optimized, our results show that the D-Phe analogues of San B inhibit *in vitro* translation by 80% at concentrations similar to their IC<sub>50</sub> values.

Protein synthesis, cell growth, and cell cycle progression are tightly coupled events.<sup>8a</sup> Many ribosomal proteins contribute extra ribosomal functions that can affect both gene transcription and translation.<sup>12</sup> Protein L7 (from the 60S subunit) is overexpressed in colorectal cancers, causes cell cycle arrest, and induces apoptosis.<sup>8a,13</sup> Our data show that all three compounds (**2**, **3**, and **4**) are cytotoxic to the colon cancer cell line and they bind to ribosomal subunits including L7.

Thus, we anticipate that the San B derivatives would halt DNA synthesis and induce apoptosis. To measure the impact of the San B analogues on DNA synthesis, we measured BrdU incorporation in HCT-116 cells when treated with **2**, **3**, or **4** (Figure S3).<sup>6</sup> Our data suggest that compound **4** has a significant inhibitory effect on DNA synthesis. To analyze the mechanism of growth inhibition, we examined cell morphology, caspase 3/7 activity (Figure S2),<sup>6</sup> and cell permeability of HCT-116 cells

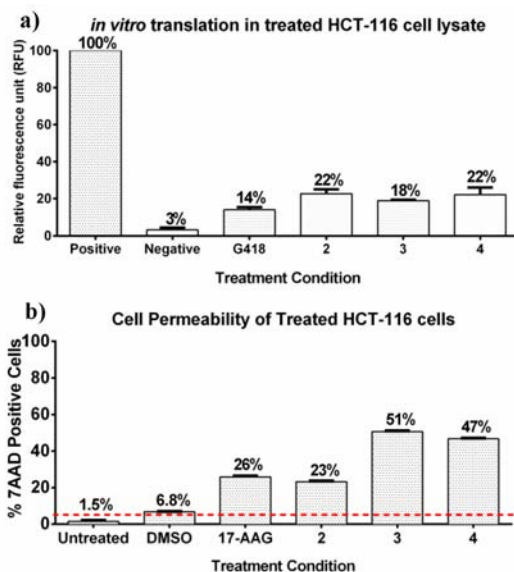


**Figure 2.** (a) Cell-free based *in vitro* translation assay. Positive (Fully translated proteins), Negative (No protein production), G418 (5  $\mu$ M), **2** (50  $\mu$ M), **3** (50  $\mu$ M), **4** (20  $\mu$ M). The average of five independent experiments is shown. (b) Cell membrane permeability of HCT-116 cells after 48 h of treatment, as measured by 7-AAD uptake. Compound concentrations are identical to those used in part a.

treated with San B derivatives. Treatment of cells with 40  $\mu$ M of **2** induced the formation of sickle-shaped nuclei in treated cells, a modest increase in caspase 3 activity over the DMSO control, and 23% of **2**-treated cells were permeable as measured by 7-AAD incorporation (Figures 2b, 3C, and S2). These results point to autophagy as the primary mechanism for **2**-mediated growth inhibition.

Autophagy is a cellular defense mechanism whereby cells degrade cytoplasmic molecules and misfolded proteins when the proteasome degradation pathway is compromised and/or the endoplasmic reticulum is undergoing stress.<sup>14</sup> Cellular components are degraded in large autophagic vacuoles called autophagosomes, and cells can utilize this mechanism to replenish amino acids and maintain homeostasis. There is a degree of overlap between the pathways that control autophagy and those that induce apoptosis, and caspase 3 can be detected in autophagic cells.<sup>15</sup> Since **2** binds to ribosomal proteins and inhibits translation, we believe that **2** causes endoplasmic reticulum stress and leads to the induction of autophagy within 48 h.

Treatment of cells with 40  $\mu$ M of **3** induced 51% cell permeability over the DMSO control as measured by 7-AAD staining (Figure 2b). Interestingly, the cell morphology

(11) Eustice, D. C.; Wilhelm, J. M. *Antimicrob. Agents Chemother.* **1984**, 26, 53.

(12) Lindström, M. S. *Biochem. Biophys. Res. Commun.* **2009**, 379, 167.

(13) (a) von Mikecz, A.; Hemmerich, P.; Peter, H.-H.; Krawinkel, U. *Immunobiology* **1994**, 192, 137. (b) Kasai, H.; Nadano, D.; Hidaka, E.; Higuchi, K.; Kawakubo, M.; Sato, T. A.; Nakayama, J. *J. Histochem. Cytochem.* **2003**, 51, 567. (c) Neumann, F.; Hemmerich, P.; Vonmikecz, A.; Peter, H. H.; Krawinkel, U. *Nucleic Acids Res.* **1995**, 23, 195.

(14) Zheng, H.-y.; Zhang, X.-y.; Wang, X.-f.; Sun, B.-c. *Differentiation* **2012**, 4, 11.

(15) Bursch, W.; Karwan, A.; Mayer, M.; Dornetshuber, J.; Frohwein, U.; Schulte-Hermann, R.; Fazi, B.; Di Sano, F.; Piredda, L.; Piacentini, M.; Petrovski, G.; Fesus, L.; Gerner, C. *Toxicology* **2008**, 254, 147.

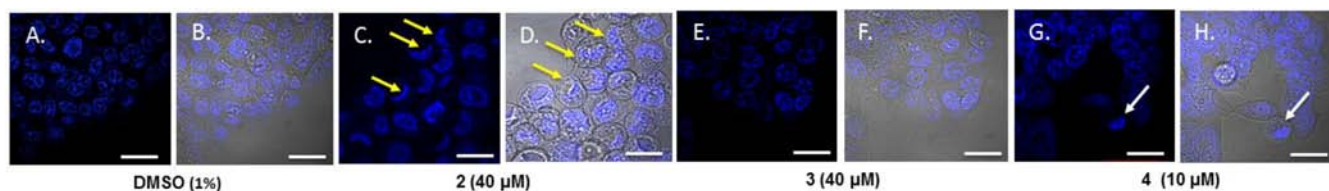


**Figure 3.** Morphological analysis of HCT-116 cells treated for 48 h with San B derivatives or DMSO. Confocal microscopy (100 $\times$ ) images show DNA staining (DAPI; A, C, E, G) or the merged image (DAPI+DCI; B, D, F, H). White arrows indicate cell rounding. Yellow arrows indicate sickle-shaped nuclei. White bars indicate 40  $\mu$ m.

data (Figure 3E and F) indicated no cell rounding or DNA condensation at 48 h after treatment, although 51% of the cells are permeable. These data indicate that **3** induces necrosis in treated cells, and this mode of cell death predominates in **3**-treated cells.

We hypothesized that **3** may induce a Type II'  $\beta$ -turn that would allow the nonpolar face of the molecule (valine, alanine, thiazole) to insert itself into the lipid bilayer of the plasma membrane and enhance membrane permeability. The Type II'  $\beta$ -turn is a key feature of Gramicidin S, which is an amphiphilic molecule. Gramicidin S forms an anti-parallel  $\beta$ -sheet that inserts itself into lipid bilayers.<sup>16</sup> The high level of cell permeability induced after treatment with **3**, combined with the lack of cell rounding or DNA condensation observed in apoptotic cells, would strongly support our hypothesis that **3** induces necrosis by a mechanism that is similar to Gramicidin S.

Treatment of HCT-116 cells with 10  $\mu$ M of **4** induced a 2-fold increase in caspase 3/7 activity over the DMSO control (Figure S2).<sup>6</sup> Cells treated with **4** (10  $\mu$ M) or the pro-apoptotic molecule 17-AAG (1  $\mu$ M) were round in appearance, with condensed chromatin (compare Figure 3G and H with Figure S1). In addition, 47% of **4** treated cells were permeable, as measured by incorporation of 7-amino-actinomycin D (7-AAD) (Figure 2b). These results, in combination with the cell morphology data, indicate that compound **4** induces apoptosis by a caspase 3 pathway. The large degree of membrane permeability suggests that the majority of **4**-treated cells are undergoing secondary necrosis at 48 h, which occurs after the induction of apoptosis.

In conclusion, our data indicate that the D-Phe analogues of San B bind to ribosomal subunits, yet the

mechanism of growth inhibition induced by each derivative is dependent on the position of the D-Phe. Ribosome binding and inhibition have been seen in other thiazole-containing macrocyclic peptides, including thiocillin and Marthiapeptide A.<sup>17</sup> Thus, our data are consistent with those of others, although Sanguinamide B contains the unique structural feature of a 4,2-bisheterocycle tandem, with an oxazole directly linked to a thiazole. Placing the D-Phe between the valine and thiazole to generate **2** inhibits translation, causes endoplasmic reticulum stress, and leads to the induction of autophagy. In contrast, placing the D-Phe substituent between the thiazole and proline 2 induces a Type II'  $\beta$ -turn, which leads to necrosis in compound **3** treated cells. Finally, compound **4**, which contains the D-Phe between the Cbz-lysine and thiazole, induces apoptosis via a caspase 3 pathway. We suspect that compounds **2** and **4** bind to the same site on the ribosomal machinery, but **4** is more effective at inhibiting translation because of the Cbz-lysine moiety. Studies are underway that will optimize compound **4** as a lead structure for inhibiting the ribosomal translation machinery.

**Acknowledgment.** We thank C. Brownlee and the Biological Resources Imaging Laboratory (BRIL) and UNSW for support of D.M.R., and S.R.M.

**Supporting Information Available.** Synthetic procedures, characterization data, and biological assays. This material is available free of charge via the Internet at <http://pubs.acs.org>.

(17) (a) Zhou, X.; Huang, H.; Chen, Y.; Tan, J.; Song, Y.; Zou, J.; Tian, X.; Hua, Y.; Ju, J. *J. Nat. Prod.* **2012**, *75*, 2251. (b) Aulakh, V. S.; Ciufolini, M. A. *J. Am. Chem. Soc.* **2011**, *133*, 5900.

The authors declare no competing financial interest.

(16) Prenner, E. J.; Lewis, R. N.; McElhaney, R. N. *Biochim. Biophys. Acta* **1999**, *1462*, 201.